Supporting Information

Robson et al. 10.1073/pnas.1116637109

SI Methods

Peptide Modification and Nanoparticle Conjugation. Peptides 12.1 and $12.1_{W\Delta A}$, with an N-terminal GSGS spacer, were purchased attached to Wang resin via the C terminus. The N terminus was deprotected ready for modification with BT in the solid phase, as shown in the schematic (Fig. S1). Full sequences (C–N) of peptides 12.1 and $12.1_{W\Delta A}$ are as follows: Resin-NLGE-WYDMFRPM-GSGS and Resin-NLGEAYDMFRPM-GSGS, respectively. Peptide was calculated to account for 70% of the total peptide–resin weight, and peptide-bound resin (12.14 mg of 12.1, 19.4 mg of $12.1_{W\Delta A}$) was preswelled in 1 mL of dimethylformamide (DMF) for a minimum of 30 min. A total of 1.5 eq (1.75 mg 12.1, 3.04 mg $12.1_{W\Delta A}$) *O*-(7-Azabenzotriazol-1-lyl)-*N*,*N*,*N*,*N*-tetramethyluronium hexafluorophosphate (HATU) and 3 eq (1.70 μL 12.1, 4.40 μL $12.1_{W\Delta A}$) *N*,*N*-diisopropylethylamine (DIPEA) were mixed with 1 eq BT (153.4 μL 12.1, 175.3 μL $12.1_{W\Delta A}$ of 2×10^{-2} M in DMF) and immediately added to the preswelled peptide–resin. The reaction mixture was left to stir at 20 °C for 6 h. Following removal of the reaction solution, resin was washed once with DMF (1 mL), acetonitrile (MeCN) (3 × 1 mL), and diethyl ether (DEE) (3 × 1 mL) and dried under nitrogen. A second delivery of 1 eq BT was preactivated with 1.5 eq HATU and 3 eq DIPEA in a total volume of 1.5 mL of DMF and added to the dried resin. After stirring for 16 h, the solution was discarded and resin was washed with DMF (1 mL), MeCN (3 × 1 mL), and DEE (3 × 1 mL) as described above. Modified peptides were cleaved from the resin using a 2.2-mL cleavage mixture [2 mL trifluoroacetic acid (TFA), 100 μL triisopropylsilane (TIS), and 100 μL d_2H_2O] for 4 h in an inert atmosphere. Cleaved peptide was filtered from the resin using a 1.0-μm polytetrafluoroethylene (PFTE) filter, which was washed through with MeCN (2 × 2 mL). Solvent was removed under reduced pressure, and cold DEE (1 mL) was added to afford a precipitate. Following DEE removal, the precipitate was dissolved in an appropriate volume of MilliQ-H_2O (4 mL). Unmodified peptides 12.1 and $12.1_{W\Delta A}$ were prepared by preswelling the resin for a minimum of 30 min in DMF and cleaving from resin as described for peptide–BT conjugates.

Peptide 12.1 is reported to form an α helix, and this was verified by CD in 50% Trifluoroethanol (TFE). CD results showed peptide 12.1 to have a random conformation in aqueous solution with the propensity to adopt a helical secondary structure (Fig. S2*A*). Analysis also demonstrated that the potential for peptide 12.1 to form a helical conformation is not hampered by BT conjugation (Fig. S2*B*). Peptide 12.1–BT and mutant peptide $12.1_{W\Delta A}$ demonstrated high- and low-binding affinity for the MDM2 hydrophobic cleft in a competition ELISA (Fig. S3).

Nanoparticle conjugates were characterized by extinction spectroscopy and MALDI-MS. A red shift, of ∼4 nm, of the plasmon band λ-max monitored by extinction spectroscopy (Fig. S4) shows an increase in particle size relative to the size of conjugating molecule. The red shift is more pronounced for peptide 12.1 than for peptide $12.1_{W\Delta A}$ because of the presence of tryptophan.

Successful modification of peptides 12.1 and $12.1_{W\Delta A}$ with BT was shown by MALDI-MS analysis (Fig. S5). Ions with *m*/*z* 563.9, 1,845.9, and 2,391.9 represent BT, peptide 12.1, and peptide 12.1–BT, respectively, whereas values of 1,730.7 and 2,276.3 *m*/*z* correspond to peptide $12.1_{W\Delta A}$ and peptide $12.1_{W\Delta A}$–BT. Following nanoparticle conjugation, analytes were removed from the nanoparticle surface using DTT displacement. MALDI-MS analysis of the removed analytes was used to verify presence of the peptide on the nanoparticle surface.

Characterization of PSN Assembly. SEM analysis of PSN samples with and without MDM2 shows partial aggregation of PSN-12.1 following MDM2 addition (Fig. S6). Formation of predominantly dimers and trimers provides an explanation for the small changes observed in extinction spectroscopy compared with a relatively large increase in SERS intensity.

MDM2 was replaced by BSA in the reaction mixture as an alternative control to test the biological specificity of the interaction. Extinction spectroscopy and SERS results are shown for PSN samples with a 1:1,000 ratio of PSN:protein (Fig. S7).

MDM2 Purification, MDM2 Ubiquitination Assays, and Protein-Binding ELISAs. Bacterially expressed full-length, untagged human MDM2 was expressed in *Escherichia coli* BL21 cells harboring a pT7.7 plasmid containing the MDM2 gene. The MDM2 protein was induced by addition of 1 mM final concentration of isopropyl-1-thio-D-galactopyranoside and 100 μM zinc chloride. Sedimented cells were washed with 50 mM Tris-HCl (pH 8.0), and the final pellet was resuspended to OD. 100 (optical density at 595 nm) in 10% (vol/vol) sucrose, 50 mM Tris-HCl (pH 8.0), lysozyme (150 μg/mL), Pefabloc (2 mM; Roche Molecular Biochemicals), DTT1 (5 mM; BDH Laboratory Supplies), benzamidine (1 mM), and NaCl (0.25 M final concentration). The cell suspension was incubated on ice 45 min, 37 °C for 1 min, and then returned to ice. The cells were lysed on ice by sonication and the lysate was centrifuged and filtered through a 0.22-μm Whatman syringe filter, and the supernatant was fractionated on a 5-mL HiTrap-SP column (Amersham Biosciences) equilibrated with buffer A [15% glycerol, 25 mM Hepes (pH 8.0), 0.02% Triton X-100, 5 mM DTT, and 1 mM benzamidine]. The supernatant was diluted 5× with buffer A before application onto the column, and bound protein was eluted in a 40-column volume linear gradient in buffer A from 0.05 to 1.0 M KCl. Aliquots of the fractions from the column were assayed for the purity of MDM2 by SDS gel, by Western blotting, and by specific activity. Purified MDM2 (SP fractions 25–29) was used in SERS binding. Bacterially expressed MDM2 protein was also further validated in ubiquitination assays (Fig. S8*C*), tetrameric p53 protein binding assays (Fig. S8*A*), and BOX-I p53 peptide-binding assays (Fig. S8*B*) to demonstrate that the 12.1 peptide used in SERS was bioactive in standard MDM2 activity assays.

To measure the binding of MDM2 protein to peptides or p53 in the solid phase by ELISA, 96-well plates (Costar) were coated with p53 protein (20 ng) in coating buffer [0.1 M $NaHCO_3$ (pH 8.6)] by incubation overnight at 4 °C. For p53–peptide binding, the BOX-I peptide (1 ng/well) was added to an ELISA well precoated with streptavidin in coating buffer [0.1 M $NaHCO_3$ (pH 8.6)] (500 ng/well) and prewashed with PBS-T (PBS supplemented with 0.1% Tween-20); nonspecific binding was blocked by incubation in blocking buffer (3% BSA in 1× PBS) for 1 h at room temperature After either p53 adsorption or p53–peptide capture, and washing with PBS-T (PBS supplemented with 0.1% Tween-20), nonspecific binding was blocked by incubation in blocking buffer (3% BSA in 1× PBS) for 1 h at room temperature. A titration of MDM2 was performed (without or with preincubation with ligands; Figs. S3 and S9), and the plate was incubated for 1 h at room temperature. Following further washes, the plate was incubated with primary antibody specific to MDM2 for 1 h at room temperature. After washing, the ap-

propriate HRP-conjugated secondary antibody was added and the plate was incubated for 1 h at room temperature. After final washing, binding was measured by enhanced chemiluminescence (ECL). The luminescence produced was immediately detected with a Fluoroskan Ascent FL luminometer and Ascent software version 2.4.1 (Labsystems).

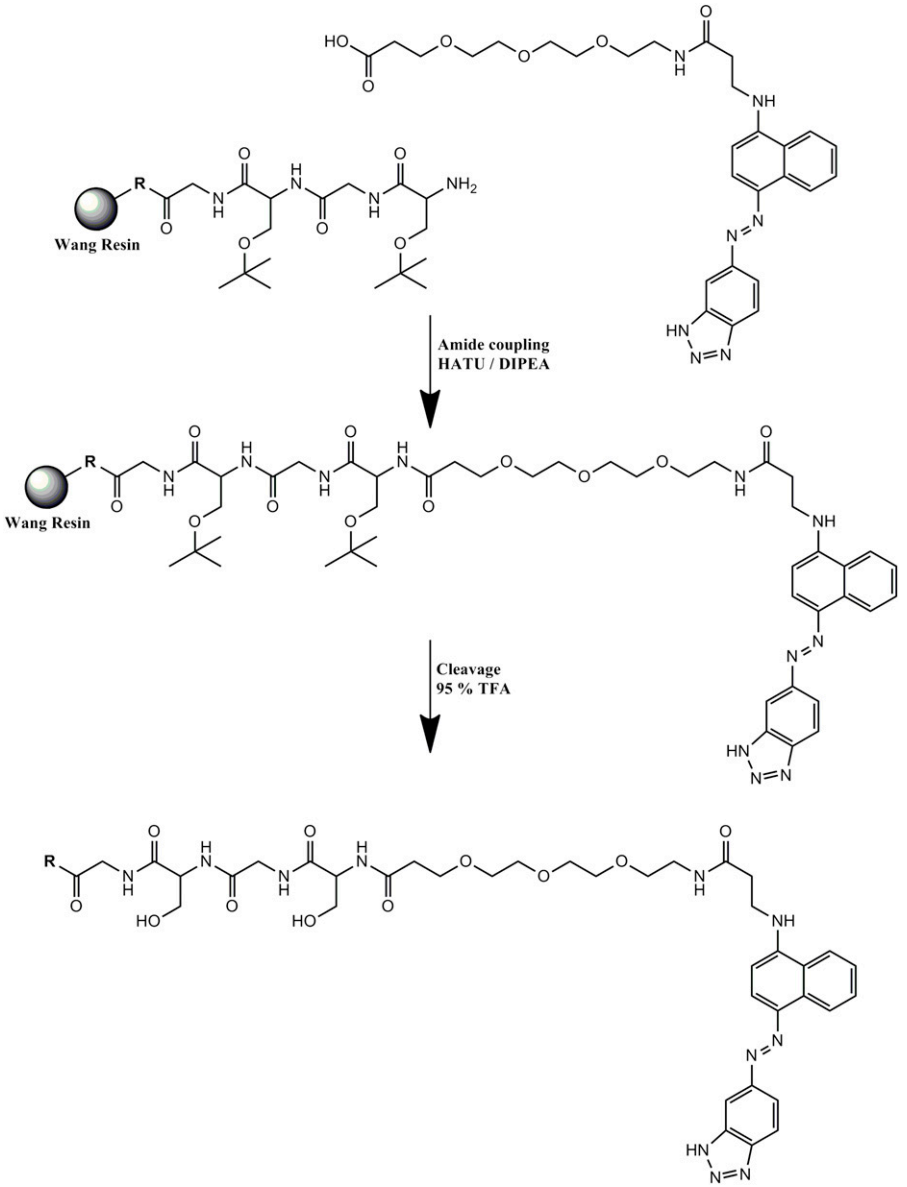

Fig. S1. Schematic of peptide–BT modification procedure where R can represent either peptide 12.1 or peptide $12.1_{W\Delta A}$.

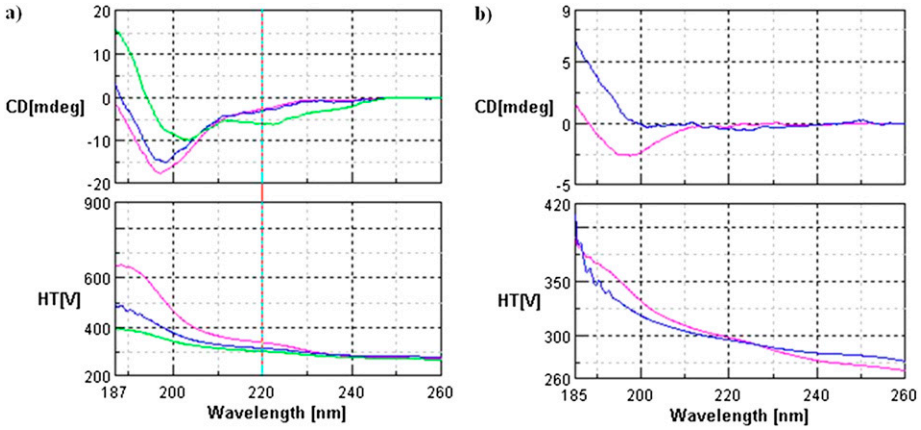

Fig. S2. (*A*) Far UV CD spectra of unmodified peptide 12.1 in H_2O (pink) in 10% TFE (blue) and 50% TFE (green). (*B*) Far UV CD spectra of peptide 12.1-BT in H_2O (pink) and 50% TFE (blue).

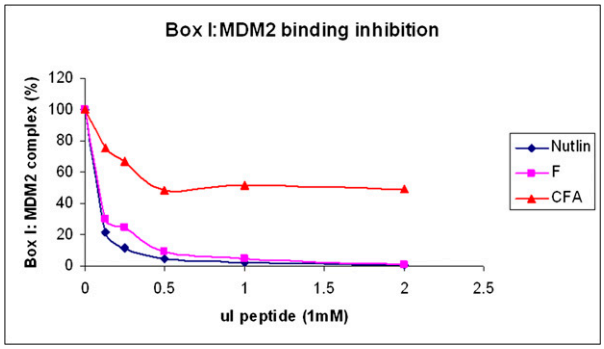

Fig. S3. Competitive inhibition of MDM2-binding to p53-derived BOX-I peptides by ligands. Competitive ELISAs that measure the binding between full-length MDM2 and p53-derived BOX-I peptide ligand were performed as described previously (1). Biotinylated p53-BOX-I peptide was adsorbed to a streptavidin-coated ELISA well, and fixed levels of MDM2 were added into a buffer with increasing amounts of the indicated ligand; peptide 12.1, mutant peptide $12.1_{W\Delta A}$, and Nutlin-3. Peptide 12.1 and mutant peptide $12.1_{W\Delta A}$ are represented by F and CFA respectively. Reaction solutions were added to the ELISA well and incubated for 1 h at room temperature. Binding of MDM2 was quantified using an anti-MDM2 MAb and secondary antibody coupled ot peroxidase, as indicated (1). The data demonstrate that peptide 12.1 is almost as potent as Nutlin-3 in displacing MDM2 from p53.

1. Worrall EG, et al. (2009) Regulation of the E3 ubiquitin ligase activity of MDM2 by an N-terminal pseudo-substrate motif. *J Chem Biol* 2:113–129.

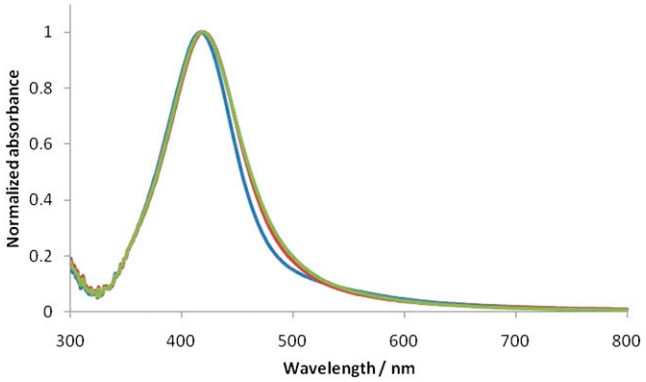

Fig. S4. Extinction spectroscopy of AgEDTA conjugates. Plasmon band λ-max of conjugates are 416 (AgEDTA), 421 (PSN-12.1), and 419 (PSN-$12.1_{W\Delta A}$).

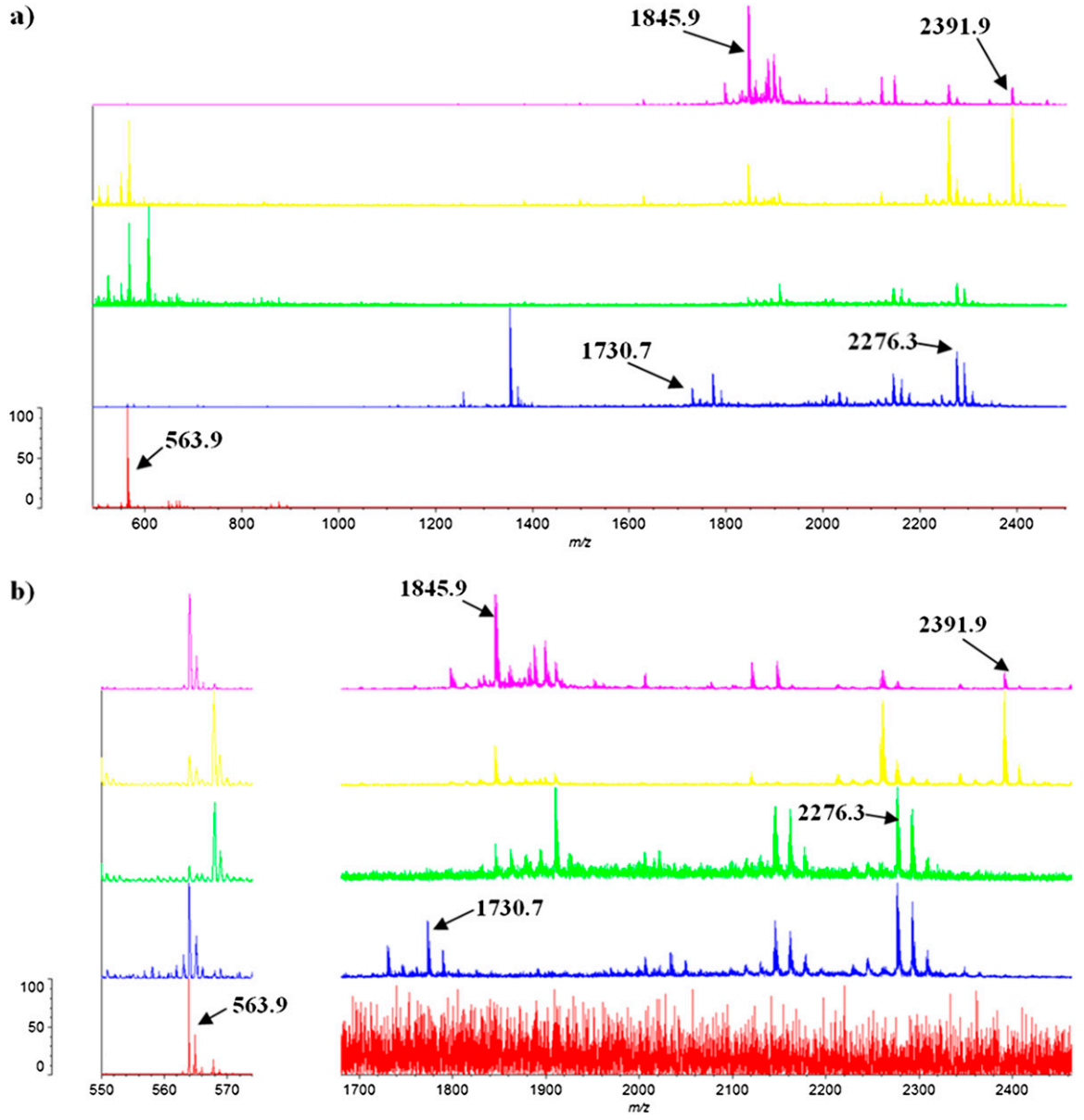

Fig. S5. MALDI-MS analysis [entire spectra (*A*) and magnified regions (*B*)] of peptide 12.1–BT (purple), peptide 12.1–BT removed from nanoparticles (yellow), peptide $12.1_{W\Delta A}$–BT (green), peptide $12.1_{W\Delta A}$–BT removed from nanoparticles (blue) and BT removed from nanoparticles (red).

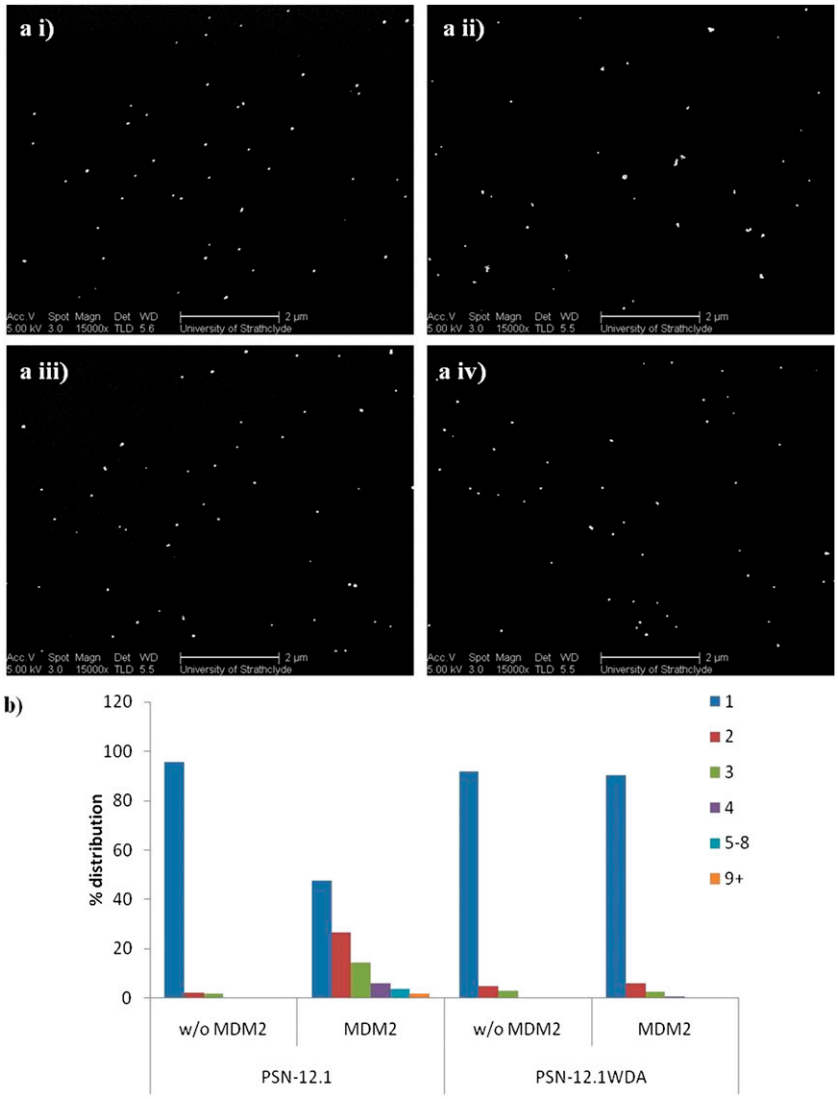

Fig. S6. (*A*) SEM images of PSN-12.1 (*i*), PSN-12.1-MDM2 (*ii*), PSN-12.1$_{W\Delta A}$ (*iii*), and PSN-12.1$_{W\Delta A}$-MDM2 (*iv*). (*B*) Statistics from SEM analysis showing the percentage of different size clusters. Numbers in the legend represent the number of PSNs per cluster.

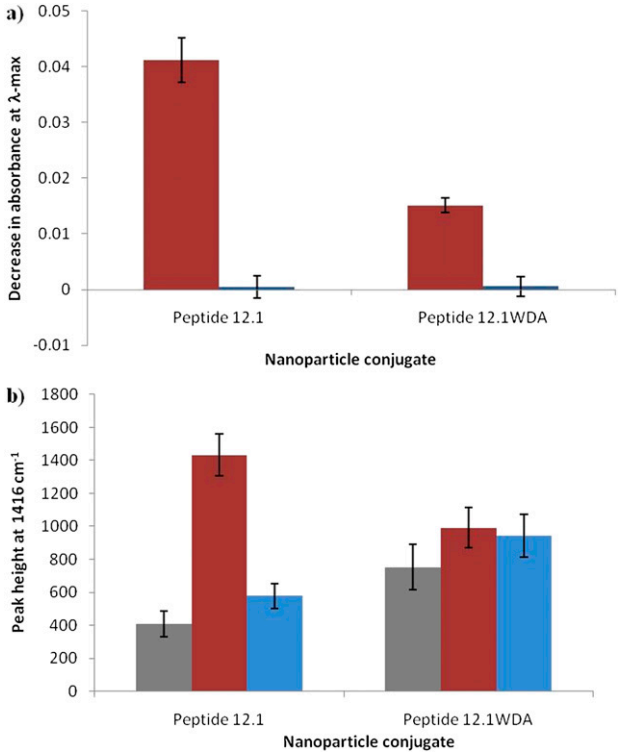

Fig. S7. Extinction spectroscopy (*A*) and SERS analysis (*B*) of PSN before and after the addition of MDM2/BSA.

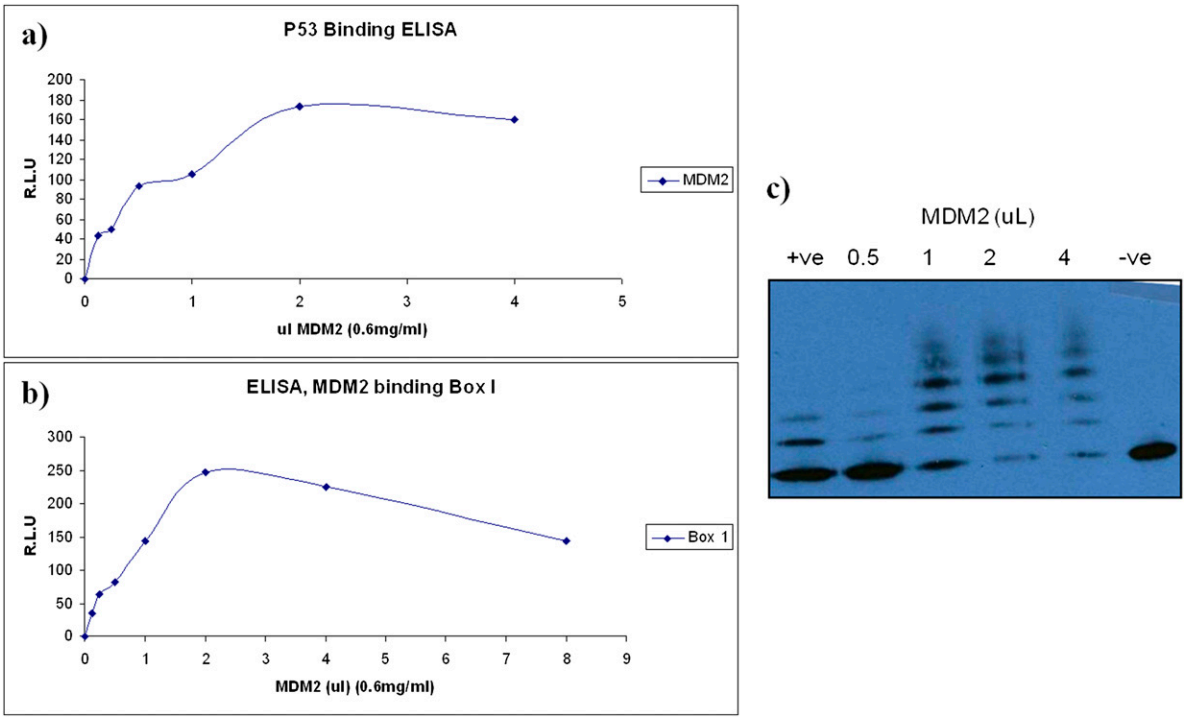

Fig. S8. Validation of MDM2 protein-specific activity. (*A*) p53 protein binding. Tetrameric full-length p53 was bound to the solid phase, and the indicated amounts of MDM2 protein were titrated into ELISA wells to measure the activity of MDM2 protein. The data are plotted as MDM2-binding activity toward p53 (in relative light units) as a function of MDM2 titration. (*B*) p53-BOX-I peptide binding. The biotinylated p53 peptide was captured on streptavidin-coated ELISA wells, and the indicated amounts of MDM2 protein were titrated into ELISA wells to measure the activity of MDM2 protein. The data are plotted as MDM2-binding activity toward p53 (in relative light units) as a function of MDM2 titration. (*C*) MDM2 activity as an E3 ubiquitin ligase. Reactions contained 25 mM Hepes (pH 8.0), 10 mM MgCl2, 4 mM ATP, 0.5 mM DTT, 0.05% (vol/vol) Triton X-100, 0.25 mM benzamidine, 10 mM creatine phosphate, 3.5 units/mL creatine kinase, ubiquitin (2 μg), E1 (50–200 nM), E2 (0.1 μM), p53 (100 ng), and human MDM2 (50 ng). Reaction products were analyzed by immunoblotting for changes in p53 mass, and the ubiquitin adducts can be observed by the multiple bands (from left lanes 3–5 vs. 1, 2, and 6).

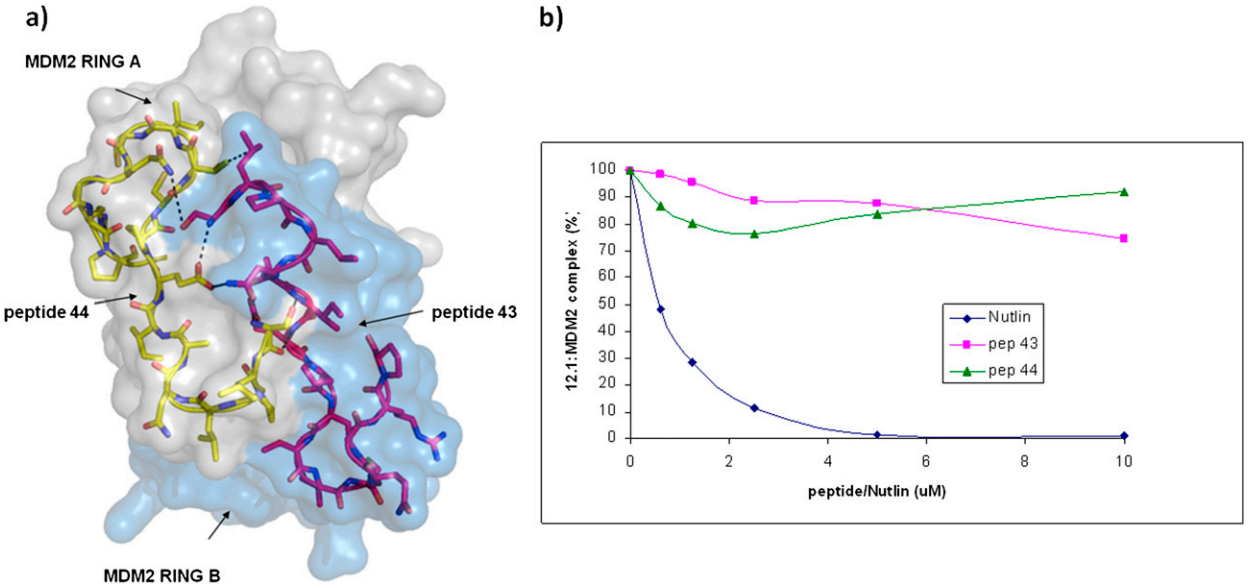

Fig. S9. Illustration of the dimerization interface peptide interactions and verification that these interactions do not affect N-terminal-binding activity. (*A*) The structure of the dimeric MDM2/MDM2 RING domain [Protein Data Bank (PDB) code 2HDP] is depicted, with stabilizing interdomain interactions highlighted from the dimer interface of the MDM2/MDMX heterodimer (PDB code 2VJF) (1). One interface peptide (peptide 44; PLNAIEPCVICQGRP) in yellow (arrow) and the N terminus of the junction interface (peptide 43; DKEESVESSLPLNAI) in red (arrow) of which the latter has its N terminus outwith the structure. (*B*) Competitive ELISA used to measure the binding between full-length MDM2 and peptide 12.1 (2). Biotinylated peptide 12.1 was adsorbed to a streptavidin-coated ELISA well, and fixed levels of MDM2 were added into a buffer with increasing amounts of the indicated ligand: Nutlin-3, RING-binding peptide 43, and RING-binding peptide 44. Reaction solutions were added to the ELISA well and incubated for 1 h at room temperature. Binding of MDM2 was quantified using an anti-MDM2 MAb and secondary antibody coupled to peroxidase, as indicated (2). The data demonstrate that RING-binding peptides 43 and 44 do not interfere with MDM2 N-terminal binding to peptide 12.1.

1. Linke K, et al. (2008) Structure of the MDM2/MDMX RING domain heterodimer reveals dimerization is required for their ubiquitylation in trans. *Cell Death Differ* 15:841–848.
2. Worrall EG, et al. (2009) Regulation of the E3 ubiquitin ligase activity of MDM2 by an N-terminal pseudo-substrate motif. *J Chem Biol* 2:113–129.